# WYPiWYG hyperelasticity without inversion formula: application to passive ventricular myocardium

Marcos Latorre[a], Francisco J. Montáns[a,*]

[a]*Escuela Técnica Superior de Ingeniería Aeronáutica y del Espacio, Universidad Politécnica de Madrid, Madrid, Spain*

**Abstract**

WYPiWYG hyperelasticity is a family of computational procedures for determining the stored energy density of soft materials. Instead of assuming the global analytical shape of these functions (the model), they are computed solving numerically the differential equations of a complete set of experimental tests that uniquely define the material behavior. WYPiWYG hyperelasticity traditionally uses an inversion formula to solve the differential equations, which limits the possible types of tests employed in the procedure. In this work we introduce a new method that does not need an inversion formula and that can be used with any type of tests. We apply the new procedure to determine the stored energy function of passive ventricular myocardium from five experimental simple shear tests.

*Keywords:* Hyperelasticity, Soft materials, Myocardium, Biological tissues, Splines.

## 1. Introduction

Finite element analysis is a widely known, powerful numerical method employed to solve numerically general boundary value problems [1]. Since its development in the mid-20th Century, it has replaced many analytical methods, often based on *assumed shapes* of the solution to the problem. Finite elements, as other modern numerical methods, do not assume the shape of the overall solution, but compute it using pre-defined *local interpolations* between nodal solutions.

*Corresponding author

*Email addresses:* m.latorre.ferrus@upm.es (Marcos Latorre), fco.montans@upm.es (Francisco J. Montáns)

Rubber-like materials [2] and soft biological tissues [3], frequently analyzed with finite elements [1], present a highly nonlinear behavior often considered as hyperelastic [4]. Hyperelastic behaviour assumes the existence of a stored energy function such that no dissipation occurs during cyclic loading. The stored energy function cannot be measured and the analytical solution obtained directly from the measured stress-strain behavior needs some integrability conditions difficult to fulfill. The typical solution to determine the stored energy is not different in essence to many other semi-inverse methods employed to solve boundary value problems before the finite elements era. As in the Rayleigh method in structures, the classical hyperelastic model simply consists in the assumption of a possible analytical stored energy function, leaving free some material parameters. These parameters are then obtained as to best-fit the measured stress-strain behavior [9]. In essence, the parameters represent the closest solution to the actual stored energy in the predefined reduced space of global solutions, or at least they represent its effects on the available tests. The procedure to obtain these parameters is often not straightforward, and an extensive variety of optimization algorithms is employed. Remarkably, the solution obtained is not unique because the problem may not have a unique minimum [6]. The different non-unique material parameter solutions may result in very different finite element predictions in general boundary value problems, as largely reported in the literature [10], [11], [12]. We remark that the actual reason for this lack of confidence in finite element solutions is the use of an insufficient number and variety of tests to properly define the material behavior under the general loading condition that may be found at integration points during finite element simulations [6], [5]. If a complete set of tests is employed, it is expected that the obtained numerical solutions are similar in these circumstances [6], [13], at least under moderately large strains.

What-You-Prescribe-Is-What-You-Get (WYPiWYG) hyperelasticity is a different, purely numerical approach, to the problem of determining the stored energy function of a hyperelastic material that exactly replicates a complete set of experimental data presented to the model. It is, in some sense, similar to finite elements in solving a general boundary value problem. The WYPiWYG approach does not specify the global shapes of the stored energy terms, but computes them numerically. It does not employ material parameters. The solution is unique, explicit, without the need of any optimization procedure. Furthermore, it may be exact to machine precision if desired. The basic idea is to compute the solution of the stored energy by means of *local* shape functions, which interpolate numerical (nodal) values of the derivative of the stored energy terms. The computation of these nodal values is the purpose of the numerical procedure. Of course, once the stored energy is obtained, it may be employed with confidence in predictions of other boundary conditions em-

ploying finite elements as if the stored energy was an analytical single continuous function because, in short, it is an analytical piecewise function with the required smoothness. In fact, we have shown in Ref. [13] that for the isotropic case, if the procedures are fed with "experimental" data (i.e. stress-strain curves) from an analytical model fulfilling the Valanis-Landel decomposition, the ulterior WYPiWYG predictions under arbitrary loadings are equal to those obtained by the analytical model. In essence, we have numerically solved the differential equations of the experiments to obtain the true solution in piecewise form. Both the results for nonhomogeneous problems and the equilibrium iterations are the same. The computational cost is also comparable.

The WYPiWYG formulations have been developed from the ideas given in the model of Sussman and Bathe [14], which is the first WYPiWYG model. The Sussman and Bathe model for isotropic incompressible hyperelasticity employs piecewise cubic interpolation functions. In order to obtain the nodal values, they used the Kearsley and Zapas (KZ) inversion formula [15]. This formula is the analytical solution to the stored energy derivative for materials fulfilling the Valanis-Landel decomposition [16]. The KZ formula is a convergent series. Usually 20-50 terms are needed to reach the machine precision at the nodes. Between nodes the accuracy depends obviously on the number of nodes, but cubic splines require few nodes to reach indistinguishable solutions. In previous works we have extended the computational procedure to account for transverse isotropic [17] and orthotropic [18] incompressible materials using a Valanis-Landel-type decomposition equivalent to the one employed under infinitesimal deformations. In these works it was necessary to develop a more general inversion formula to solve the differential equations. In [13] we extended the procedure for compressible materials and we have shown that it is in fact a natural, equation-by-equation, extension of an infinitesimal framework accounting for bilinear behavior (with possible different moduli in tension and compression). The method can be considered as "model-free", "data-based" hyperelasticity.

One of the important features of WYPiWYG hyperelasticity, in contrast to many popular models, is that it recovers the full linear theory even in the orthotropic case. Obviously it is desirable that for infinitesimal deformations, the infinitesimal theory is recovered [21], [22], [23] and also desirable that this happens at any strain level, because every incremental (infinitesimal) deformation, even at large strains, can be considered as an infinitesimal case over a deformed configuration. From a practical point of view this also implies that engineering judgment inherited from the infinitesimal theory may be employed in the analysis of large strain models. For example, missing experimental data needed to uniquely define the material behavior may be assumed based on that experience, as for example Poisson ratios [5] (see also

[24]). Experimental evidence has proved the adequacy of these hypotheses [25].

The predictive capabilities of the WYPiWYG method are excellent. It has been shown that it is capable of predicting the behaviour of a large variety of materials to high accuracy; arteries in [5], superficial fascia in [20], skin in [19], incompressible rubber in [6] and compressible polyurethane foam in [13]. We will show also below excellent predictions for the passive myocardium experiments of Dokos et al. [26]. The models have been implemented in finite element codes (Dulcinea and Adina) and tested for nonhomogeneous deformations in some of these works.

One of the major difficulties in WYPiWYG hyperelasticity is that, in most practical cases, we need to solve the differential equations of the experiments by means of an inversion formula, but this is not always possible. Then, the procedure lacks a desired generality. The purpose of this paper is to generalize the WYPiWYG procedure as to bypass the need of an inversion formula, or any other add-hoc solution, and bring a procedure of more general applicability. With the new procedure proposed herein, the differential equations from any complete set of tests, uniquely defining the material behavior, can be solved numerically, obtaining therefore an also unique stored energy density in the proposed uncoupled form that "exactly" (to any desired precision) predicts the experimentally observed stress-strain behavior.

In the next section we briefly review the piecewise spline interpolation equations and recast the interpolation in a new convenient form for our purpose. Thereafter we explain the new, yet simple computational procedure. Finally we use that procedure to predict the experimental results on passive myocardium from Dokos et al [26]. We also note that the set of tests in Dokos et al [26] is incomplete because there are infinite stored energies even in uncoupled form, and compatible with the infinitesimal theory, that exactly predict the measured stress-strain behavior in such tests. Therefore, for our purpose, we complete the set of tests with reasonable assumptions to obtain a unique stored energy solution which preserves all independent deformation modes of the infinitesimal theory, and which can be further used with confidence in finite element predictions.

## 2. Piecewise spline functions in matrix form

Although different interpolation functions are possible, and may be more adequate in some cases, the piecewise cubic splines have some desirable properties of continuity and the determination is quite simple, see Refs. [17] and [18] for uniform and non-uniform spaced data sets, respectively. For the matter of notation simplicity, and without loss of generality of the procedure explained, we address herein the case with uniform spacing.

Assume that we have a set of known points $\{x_i, y_i\}$, $i = 1, ..., N+1$, that are to be interpolated by means of cubic polynomials forced to fulfill some smoothness conditions. It is convenient to normalize each subdomain $[x_i, x_{i+1}]$ defining a new normalized variable within that subdomain

$$\xi_i(x) = (x - x_i) / (x_{i+1} - x_i) \in [0, 1] \tag{1}$$

Then, each polynomial $p_i(\xi_i(x))$, $i = 1, ..., N$, is defined in the unit-length $i-th$ subinterval as

$$p_i(\xi_i) = a_i + b_i\xi_i + c_i\xi_i^2 + d_i\xi_i^3 \text{ with } 0 \leq \xi_i \leq 1 \text{ and } i = 1, ..., N \tag{2}$$

where $N$ is the number of intervals. For each subdomain $y_i = p_i(\xi = 0)$ and $y_{i+1} = p_i(\xi = 1)$. Between the current interval and the previous and subsequent ones, continuity of the first and second derivatives, which we denote by $Y_i$ and $Y_i'$ respectively, is also enforced; mathematically —note the abuse of notation in $p_i(x) = p_i(\xi(x)) = p_i(\xi)$

$$\begin{cases} p_{i-1}'(\xi_i = 1) = p_i'(\xi_i = 0) =: Y_i \\ p_{i-1}''(\xi_i = 1) = p_i''(\xi_i = 0) =: Y_i' \end{cases} \tag{3}$$

where the accent $(\cdot)'$ implies derivative with respect to the basic variable $x$, i.e. $p_i' = (dp_i/d\xi_i)/h$. However, we note that in the case herein addressed for simplicity all intervals have the same length, so $h := (x_{i+1} - x_i) = (x_i - x_{i-1})$, which cancels out in the previous equations. It is straightforward to obtain the coefficients of the polynomials as a function of $y_i$ and $Y_i$ from Eqs. (2) and $(3)_1$

$$i = 1, ..., N \begin{cases} a_i = y_i \\ b_i = Y_i \\ c_i = 3(y_{i+1} - y_i) - 2Y_i - Y_{i+1} \\ d_i = 2(y_i - y_{i+1}) + Y_i + Y_{i+1} \end{cases} \tag{4}$$

and substitute them in Eq. $(3)_2$ in order to express it in terms of values $y_i$ and $Y_i$

$$Y_{i-1} + 4Y_i + Y_{i+1} = -3y_{i-1} + 3y_{i+1}, \quad i = 2, ..., N \tag{5}$$

Note that $y_i$ are the known values being interpolated, whereas $Y_i$ are the derivatives to be determined. Once the $Y_i$ have been computed, Eqs. (4) give the polynomials. The $N-1$ Equations (5) include $N+1$ unknowns $Y_i$, because the end derivatives are not defined. There are several options to define such end derivatives. We use

herein the so-called "not-a-knot" end conditions, which give the following additional equations

$$-Y_1 + Y_3 = 2y_1 - 4y_2 + 2y_3 \tag{6}$$
$$-Y_{N-1} + Y_{N+1} = 2y_{N-1} - 4y_N + 2y_{N+1} \tag{7}$$

These $N+1$ equations may be written in a convenient matrix format as

$$\begin{bmatrix} Y_1 \\ Y_2 \\ \vdots \\ Y_N \\ Y_{N+1} \end{bmatrix} = \underbrace{\begin{bmatrix} -1 & 0 & 1 & & \\ 1 & 4 & 1 & & \\ & \ddots & \ddots & \ddots & \\ & & 1 & 4 & 1 \\ & & -1 & 0 & 1 \end{bmatrix}^{-1} \begin{bmatrix} 2 & -4 & 2 & & \\ -3 & 0 & 3 & & \\ & \ddots & \ddots & \ddots & \\ & & -3 & 0 & 3 \\ & & 2 & -4 & 2 \end{bmatrix}}_{[B]_{(N+1)\times(N+1)}} \begin{bmatrix} y_1 \\ y_2 \\ \vdots \\ y_N \\ y_{N+1} \end{bmatrix} \tag{8}$$

i.e.

$$\{Y\}_{N+1} = [B]_{(N+1)\times(N+1)} \{y\}_{N+1} \tag{9}$$

Using this solution, the coefficient Eqs. (4) may be recast as

$$\{a\}_N = [1]_{N\times(N+1)} \{y\}_{N+1} =: [A] \{y\}_{N+1} \tag{10}$$
$$\{b\}_N = [B]_{N\times(N+1)} \{y\}_{N+1} =: [B] \{y\}_{N+1} \tag{11}$$
$$\{c\}_N = [C]_{N\times(N+1)} \{y\}_{N+1} =: [C] \{y\}_{N+1} \tag{12}$$
$$\{d\}_N = [D]_{N\times(N+1)} \{y\}_{N+1} =: [D] \{y\}_{N+1} \tag{13}$$

where $[1]_{(N+1)\times(N+1)}$ is the identity matrix,

$$[C]_{N\times(N+1)} = \begin{bmatrix} -3 & 3 & & \\ & \ddots & \ddots & \\ & & -3 & 3 \end{bmatrix} - \begin{bmatrix} 2 & 1 & & \\ & \ddots & \ddots & \\ & & 2 & 1 \end{bmatrix} [B]_{(N+1)\times(N+1)} \tag{14}$$

and

$$[D]_{N\times(N+1)} = \begin{bmatrix} 2 & -2 & & \\ & \ddots & \ddots & \\ & & 2 & -2 \end{bmatrix} + \begin{bmatrix} 1 & 1 & & \\ & \ddots & \ddots & \\ & & 1 & 1 \end{bmatrix} [B]_{(N+1)\times(N+1)} \tag{15}$$

Then, we have determined the polynomials in Eq. (2)

$$\{p(\xi)\}_N = \begin{bmatrix} p_1(\xi) \\ \vdots \\ p_N(\xi) \end{bmatrix} = \{a\}_N + \xi\{b\}_N + \xi^2\{c\}_N + \xi^3\{d\}_N \tag{16}$$

$$= \left(1[A] + \xi[B] + \xi^2[C] + \xi^3[D]\right)\{y\}_{N+1} =: [P(\xi)]\{y\}_{N+1} \tag{17}$$

where the local coordinate $\xi$ is in the applicable interval $I \subset [1, N]$ and $[P(\xi)]$ is a $N \times (N+1)$ matrix including the following $N \times (N+1)$ *shape* polynomials (i.e. local cubic polynomials)

$$P_{ij}(\xi) = A_{ij} + B_{ij}\xi + C_{ij}\xi^2 + D_{ij}\xi^3 \; ; \quad i = 1, ..., N \; ; \quad j = 1, ..., N+1 \tag{18}$$

$\{y\}$ are the *nodal* values (i.e. the $N+1$ ordinates at the $N+1$ break points $\{x\}$) and $\{p(\xi)\}$ represents the *interpolated* solution (i.e. the resulting $N$ interpolation cubic splines). In index form, the interpolation setting is

$$p_i(\xi) = \sum_{j=1}^{N+1} P_{ij}(\xi) y_j \; , \quad i = 1, ..., N \tag{19}$$

Obviously, a polynomial evaluation may be performed at a specific value $\xi_k$ within an interval $i \equiv I(k)$, i.e.

$$\tilde{y}_k \equiv p_I(\xi_k) = a_I + b_I\xi_k + c_I\xi_k^2 + d_I\xi_k^3 = \sum_{j=1}^{N+1} P_{Ij}(\xi_k) y_j = [P_{I*}(\xi_k)]_{1\times(N+1)}\{y\}_{N+1} \tag{20}$$

where $P_{Ij}(\xi_k)$, $j = 1, ..., N+1$, are the shape function weights associated to the nodal values $y_j$ to give $p_I(\xi_k)$ as a result, and $[P_{I*}(\xi_k)]$ is the row $i = I$ of the $[P(\xi_k)]$ matrix, i.e.—the subscript $(I*)$ means the full row $i = I$

$$[P_{I*}(\xi_k)]_{1\times(N+1)} = \underbrace{\{A_{I*}\}}_{1\times(N+1)} + \underbrace{\{B_{I*}\xi_k\}}_{1\times(N+1)} + \underbrace{\{C_{I*}\xi_k^2\}}_{1\times(N+1)} + \underbrace{\{D_{I*}\xi_k^3\}}_{1\times(N+1)} \tag{21}$$

Consider that $N+1$ points are selected at the nodes, i.e. at locations $x_k$, so $\xi_k(x_k) = 0$ for all except the last one which is $\xi_{N+1} = 1$. Then, assemble row by row a [Π] matrix

such that the row $k$ of $[\Pi]$ is $[P_{I*}(\xi_k)]$. It is easily verified that

$$[\Pi]^{-1}_{(N+1)\times(N+1)} \{\tilde{y}\}_{N+1} \equiv \{y\}_{N+1} \tag{22}$$

i.e. we recover the nodal values $y_i$. In the case of other $N+1$ selected points $\xi_k$, we would obtain the nodal values such that the spline set has the desired values at the given locations. If we have less nodes than evaluation points $N_k$ (more nodes than evaluation points yields an ill-conditioned problem) with known ordinates $\{\hat{y}\}_{N_k}$, then the solution is not exact and must be computed in a mean squares sense, taking the minimum norm of

$$\{R\}_{N_k} := \{\hat{y}\}_{N_k} - \{\tilde{y}\}_{N_k} = \{\hat{y}\}_{N_k} - [\Pi]_{N_k\times(N+1)} \{y\}_{N+1} \tag{23}$$

so

$$\{y\}_{N+1} = \left([\Pi]^T [\Pi]\right)^{-1}_{(N+1)\times(N+1)} [\Pi]^T_{(N+1)\times N_k} \{\hat{y}\}_{N_k} \tag{24}$$

where $[\Pi]$ is a matrix assembled with the corresponding rows $[P_{I*}(\xi_k)]$ of $[P(\xi)]$. However, we note that since the operations of spline-interpolation and discretization are immediate, the preferred choice, whenever possible, is $N_k = N+1$ and the evaluation points given at the nodes.

## 3. Incompressible isotropic material

The Valanis-Landel decomposition [16] is implicitly employed at small strains, is mathematically accurate at least up to moderately large strains [4], it is employed by many hyperelastic models, and it has been experimentally verified in many materials [4], [2]. Furthermore, if a material model fails to fulfill the Valanis-Landel decomposition, then the inherent coupling implies that a tension-compression test curve is in principle not sufficient to characterize the material [6]. Therefore, we here consider an isotropic incompressible material fulfilling the Valanis-Landel decomposition

$$\mathcal{W}(\boldsymbol{E}) = \omega(E_1) + \omega(E_2) + \omega(E_3) \tag{25}$$

where $\omega(E)$ is the scalar-valued function to be determined and $E_i$ are the principal components of the isochoric logarithmic strain tensor $\boldsymbol{E}$ in the reference configuration. These strains are constrained by the incompressibility condition $E_1+E_2+E_3 = 0$. In the practical quasi-incompressible case used in finite elements, the deviatoric strains $E_i^d = E_i - 1/3(E_1+E_2+E_3)$ are to be used, a volumetric term must be added and mixed finite element formulations are needed. In the perfectly incompressible case, it is usual to work directly with the total strains because $E_i \equiv E_i^d$.

In our procedure, $\omega(E)$ is never computed nor needed, we just need the derivative values $\omega'(E)$, so this is the actual variable. Then, using again an abuse of notation, we write $\omega_i'(E) \equiv \omega_i'(\xi_i(E)) \equiv \omega_i'(\xi_i)$, i.e. $\omega'$ is the value computed at $E$, or equivalently at $\xi_i(E)$, where $\xi_i$ is the normalized abscisa within the interval $i$ to which $E$ belongs, i.e. $\xi_i = (E - E_i)/(E_{i+1} - E_i)$. Then we can conveniently write the polynomials in terms of the normalized variable $\xi \in [0, 1]$. We interpolate the first derivative function $\omega_i'(\xi)$ in the interval $i$ as

$$\begin{aligned} \omega_i'(\xi) &= \{a\}_N + \xi\{b\}_N + \xi^2\{c\}_N + \xi^3\{d\}_N \\ &= \sum_{j=1}^{N+1} \left[A_{ij} + B_{ij}\xi + C_{ij}\xi^2 + D_{ij}\xi^3\right]\varpi_j = \sum_{j=1}^{N+1} P_{ij}(\xi)\,\varpi_j, \quad i = 1, ..., N \end{aligned} \tag{26}$$

where $\varpi_j$ are the nodal values of $\omega_i'$ at $E_j$ to be determined, and $\omega_i'(\xi)$ are the energy derivative functions, i.e. the resulting cubic polynomials within each interval. Also note that obviously $d\omega_i'/dE = h^{-1}(d\omega_i'/d\xi)$, where $h = (E_{i+1} - E_i)$ is the constant interval size.

The equilibrium differential equation during a tension-compression uniaxial test is the one that we will solve herein. This equation is

$$\sigma(E) = \omega'(E) - \omega'(-\tfrac{1}{2}E) \tag{27}$$

where $\sigma$ is the Cauchy stress, which equals the Kirchhoff stress because of the incompressibility assumption. We can evaluate this equation in as many points as the number of unknowns to be determined. The evaluation at the nodes $x_k \equiv E_k$, $k = 1, ..., N+1$, gives

$$\sigma(E_k) = \omega'(E_k) - \omega'(-\tfrac{1}{2}E_k) = \varpi_k - \omega_I'(\xi_k) = \varpi_k - \sum_{j=1}^{N+1} P_{Ij}\left(\xi_k(-\tfrac{1}{2}E_k)\right)\varpi_j \tag{28}$$

where the interval $i \equiv I(k)$ depends on the point $k$ (i.e. on $E_k$) and the corresponding normalized abscissa $\xi_k$ is

$$\xi_k(-\tfrac{1}{2}E_k) = \frac{-\frac{1}{2}E_k - E_I}{E_{I+1} - E_I} \quad \text{with } E_I \le -\tfrac{1}{2}E_k < E_{I+1} \tag{29}$$

The $N+1$ Equations (28) constitute a system of linear equations which can be

easily recast in matrix form

$$\{\sigma\}_{N+1} = [K]_{(N+1)\times(N+1)} \{\varpi\}_{N+1} \tag{30}$$

where $[K] = [1] - [\Pi]$. The row $k$ of $[\Pi]$ is assembled according to Eq. (28), i.e. $[P_{I*}(\xi_k)]$, and $[1]$ is the identity matrix. We can immediately determine the nodal unknowns $\{\varpi\}_{N+1}$ for a given experimental data set $\{\sigma\}_{N+1}$ solving this system of linear equations. Obviously the number of points employed is arbitrary, since experimental curves may be first interpolated by splines and then we can select as many points as desired. Usually the number of selected points will be smaller than the number of experimental points in a typical experimental curve, for numerical efficiency. Furthermore, we have used as many equilibrium equation evaluations as nodes being employed. However a larger amount could have been used and a minimum squares solution could be performed. Nonetheless, since the computational cost of the procedure is small, large (but reasonable, say 100 to 1000 points) discretizations do not incur in relevant penalties.

We note that we have not made use of any inversion formula. The present procedure is quite straightforward once the differential equations of the tests are given in the form of Eq. (28).

## 4. Incompressible orthotropic material

WYPiWYG incompressible orthotropic hyperelasticity is based on the following decomposition of the stored energy function

$$\mathcal{W}(\boldsymbol{E}, \boldsymbol{a}_1, \boldsymbol{a}_2) = \mathcal{W}_{iso}(\boldsymbol{E}) + \mathcal{W}_{orth}(\boldsymbol{E}, \boldsymbol{a}_1, \boldsymbol{a}_2) \tag{31}$$

where $\mathcal{W}_{iso}(\boldsymbol{E})$ is an isotropic contribution and $\mathcal{W}_{orth}(\boldsymbol{E}, \boldsymbol{a}_1, \boldsymbol{a}_2)$ is the orthotropic deviation from such contribution written in terms of the preferred material directions $\boldsymbol{a}_i$, which are perpendicular and correspond to the symmetry planes in the undeformed configuration. The model recovers the full orthotropic theory at small strains [5], [22] and fulfills the material-symmetries congruency [27]. For simplicity, and without loss of generality of the procedure, consider a vanishing isotropic contribution. The simplest orthotropic WYPiWYG stored energy is then based in the following decomposition

$$\begin{aligned} \mathcal{W}_{orth}(\boldsymbol{E}, \boldsymbol{a}_1, \boldsymbol{a}_2) = \; & \omega_{11}(E_{11}) + \omega_{22}(E_{22}) + \omega_{33}(E_{33}) + \\ & + 2\omega_{12}(E_{12}) + 2\omega_{23}(E_{23}) + 2\omega_{31}(E_{31}) \end{aligned} \tag{32}$$

where $E_{ij} = \boldsymbol{a}_i \cdot \boldsymbol{E}\boldsymbol{a}_j$ are the logarithmic strain invariants in the material preferred axes. This decomposition is identical to the one used in the infinitesimal counterpart, but written in terms of logarithmic strain components, which inherit many of the properties of the infinitesimal strains. The orthotropic model is capable of capturing independently the six independent deformation modes of the general infinitesimal theory limit; note that we have six independent energy function-components. Since the three axial functions $\omega_{ii}(E)$ have tension and compression branches, their determination usually involves six experimental loading curves. For the shear functions $\omega_{ij}(E)$ with $i \neq j$ only the positive branch must be determined (the other one is symmetric by frame invariance). Thus, in total, nine experimental curves are needed in general. Usually the terms more difficult to determine are the axial functions since they usually appear in coupled form.

Let us consider two possible sets of tests presented to the model to determine the tension-compression axial functions. The first one consist of three tension-compression test curves. This case was originally addressed in [18] and enhanced in [5], in both cases using the inversion formula. The relevant part are the axial-to-axial terms $\omega_{11}$, $\omega_{22}$ and $\omega_{33}$, because once obtained, the shear ones are determined immediately, see [18]. The second case herein studied consists of six (actually five independent) simple shear tests, to which an additional experimental or assumed curve must be added. This second case has an explicit solution, as we show below.

### *4.1. Three tension-compression uniaxial curves*

The tension curves may be obtained from tensile tests, whereas the compression curves may be obtained either from compression tests or, usually more convenient experimentally, from biaxial tests [13], [6]. Even in this case, the stored energy may be computed with several combination of curves. Consider as an example the uniaxial tension-compression curves in axes 1 and 2, respectively $\sigma_{11}(E_{11})$ and $\sigma_{22}(E_{22})$, and a curve of transverse strains $E_{22}^{(1)}(E_{11})$, where the superscript (1) indicates that the curve is obtained from the uniaxial test in direction 1. The stresses $\sigma_{11}$, $\sigma_{22}$ are the Cauchy stresses and $E_{11}$, $E_{22}$ the corresponding logarithmic strains. By incompressibility, Cauchy and Kirchhoff stresses are coincident, and for tests in preferred directions of orthotropy, generalized Kirchhoff stresses (work-conjugate to logarithmic strains in the most general anisotropic case [28]) are also coincident with Cauchy stresses.

For simplicity in this section, we assume that all tests have the same number of points, which will be also the same points used in the stored energy interpolations. The procedure can, of course, be generalized to tests with different discretizations, but note that we can always (and we usually do) interpolate and re-sample the

experimental data to obtain the same number of points. The interpolation of the $N$ spline pieces of the axial-to-axial stored energy function derivatives are —recall the abuse of notation explained before Eq. (26)

$$\left.\begin{array}{l} \omega'_{11i}\left(\xi\right)=\sum_{j=1}^{N+1}P_{ij}\left(\xi\right)\varpi_{11j} \\ \omega'_{22i}\left(\xi\right)=\sum_{j=1}^{N+1}P_{ij}\left(\xi\right)\varpi_{22j} \\ \omega'_{33i}\left(\xi\right)=\sum_{j=1}^{N+1}P_{ij}\left(\xi\right)\varpi_{33j} \end{array}\right\} \quad i=1,...,N \tag{33}$$

with $3\times(N+1)$ unknowns. The equilibrium equations for two tension-compression uniaxial tests are, for a test in direction 1 [18]

$$\sigma_{11}(E_{11})=\omega'_{11}(E_{11})-\omega'_{22}(E_{22}^{(1)}(E_{11})) \tag{34}$$

$$\omega'_{22}(E_{22}^{(1)}(E_{11}))=\omega'_{33}(E_{33}^{(1)}(E_{11})) \tag{35}$$

and for a test in direction 2

$$\sigma_{22}(E_{22})=\omega'_{22}(E_{22})-\omega'_{11}(E_{11}^{(2)}(E_{22})) \tag{36}$$

$$\omega'_{11}(E_{11}^{(2)}(E_{22}))=\omega'_{33}(E_{33}^{(2)}(E_{22})) \tag{37}$$

where the experimental data are three complete curves, say $\sigma_{11}(E_{11})$, $\sigma_{22}(E_{22})$ and $E_{22}^{(1)}(E_{11})$, e.g. $\{E_{11},\sigma_{11}\}_{N+1}$, $\{E_{22},\sigma_{22}\}_{N+1}$ and $\{E_{11},E_{22}^{(1)}\}_{N+1}$. Note also that the incompressibility conditions apply in all tests

$$\left\{\begin{array}{l} E_{11}+E_{22}^{(1)}\left(E_{11}\right)+E_{33}^{(1)}\left(E_{11}\right)=0 \\ E_{11}^{(2)}\left(E_{22}\right)+E_{22}+E_{33}^{(2)}\left(E_{22}\right)=0 \\ E_{11}^{(3)}\left(E_{33}\right)+E_{22}^{(3)}\left(E_{33}\right)+E_{33}=0 \end{array}\right. \tag{38}$$

An additional compatibility equation, that must also be fulfilled, is obtained from a fictitious test in the third direction

$$\omega'_{11}(E_{11}^{(3)}(E_{33}))=\omega'_{22}(E_{22}^{(3)}\left(E_{33}\right))\Leftrightarrow\omega'_{11}(E_{11}^{(3)}(E_{22}^{(3)}))=\omega'_{22}(E_{22}^{(3)}) \tag{39}$$

where $E_{11}^{(3)}(E_{33})$ is a function with transverse-to-axial strain coordinates $\{E_{33},E_{11}^{(3)}\}_{N+1}$

and $E_{11}^{(3)}(E_{22}^{(3)})$ is a function with transverse-to-transverse strain coordinates $\{E_{22}^{(3)}, E_{11}^{(3)}\}_{N+1}$. Both are related through Eq. $(38)_3$. In these five equations, (34) to (37) and (39), apart from the energy derivatives, two additional unknown functions of transverse strains appear, namely $E_{11}^{(2)}(E_{22})$ and $E_{11}^{(3)}(E_{33})$, and cannot be immediately reduced. Since these functions are the arguments of the spline-based strain energy terms, we do not know the specific interval that has to be assessed in order to write the governing equations directly in matrix form. However, an iterative procedure may be applied in which $E_{11}^{(2)}(E_{22})$ and $E_{11}^{(3)}(E_{33})$ are initially assumed and then iteratively corrected until convergence in $E_{11}^{(2)}(E_{22})$ and $E_{11}^{(3)}(E_{33})$ is attained, see Ref. [5].

During each iteration, we can discretize the previous five equations, i.e. Eqs. (34) to (37) and (39), and solve them simultaneously, or solve them sequentially. For the present case, our experience shows that the sequential procedure is preferred, so we detail it now. The simultaneous procedure is more straightforward to set in general for any other problem and is given in the next subsection, but requires more starting values.

For the sequential procedure, the substitution of Eq. (39) into Eq. (34) gives

$$\sigma_{11}(E_{11}) = \omega'_{11}(E_{11}) - \omega'_{11}(E_{11}^{(3)}(E_{22}^{(1)}(E_{11}))) \tag{40}$$

which is a single equation written in terms of the uniaxial strain $E_{11}$, similar to the isotropic one, in which only the energy term $\omega'_{11}$ appears. We can solve this equation in matrix form. The evaluation at the nodes $x_k \equiv E_{11k}$, $k = 1, ..., N+1$, used for the uniaxial $\sigma_{11}(E_{11k})$ curve, gives

$$\sigma_{11}(E_{11k}) = \omega'_{11}(E_{11k}) - \omega'_{11}(E_{11}^{(3)}(E_{22}^{(1)}(E_{11k}))) = \varpi_{11k} - \omega'_{11(I)}(\xi_{1k}) \tag{41}$$

$$= \varpi_{11k} - \sum_{j=1}^{N+1} P_{Ij}(\xi_{1k})\varpi_{11j} \tag{42}$$

where $I$ is the interval such that

$$E_{11(I)} \leq E_{11}^{(3)}(E_{22}^{(1)}(E_{11k})) < E_{11(I+1)} \tag{43}$$

and the normalized abscissa $\xi_{1k}$ is

$$\xi_{1k} \equiv \xi_{1k}\left(E_{11}^{(3)}(E_{22}^{(1)}(E_{11k}))\right) = \frac{E_{11}^{(3)}(E_{22}^{(1)}(E_{11k})) - E_{11(I)}}{E_{11(I+1)} - E_{11(I)}} \tag{44}$$

Recall in these last equations that $E_{22}^{(1)}(E_{11k})$ are experimental data and that the

function $E_{11}^{(3)}(E_{22}^{(3)})$ is known during the computations because it is built from the iteratively corrected transverse strains $E_{11}^{(3)}(E_{33})$ through Eq. $(38)_3$. Then, as in the isotropic case

$$\{\sigma_{11}\}_{N+1} = [K_{11}]_{(N+1)\times(N+1)} \{\varpi_{11}\}_{N+1} \tag{45}$$

where $[K_{11}] = [1] - [\Pi]$ is computed using the data corresponding to the test in direction 1. Then, since we now know the function $\omega'_{11}(E_{11})$, we obtain $\omega'_{22}(E)$ directly from Eq. (36) as

$$\omega'_{22}(E_{22}) = \sigma_{22}(E_{22}) + \omega'_{11}(E_{11}^{(2)}(E_{22})) \tag{46}$$

i.e.

$$\begin{aligned} \omega'_{22}(E_{22k}) &= \sigma_{22}(E_{22k}) + \omega'_{11(I)} \left(\xi_1(E_{11}^{(2)}(E_{22k}))\right) \\ &= \sigma_{22}(E_{22k}) + \sum_{j=1}^{N+1} P_{Ij}(\xi_1(E_{11}^{(2)}(E_{22k})))\varpi_{11j} \end{aligned} \tag{47}$$

where for each $k$

$$\xi_1 \left(E_{11}^{(2)}(E_{22k})\right) = \frac{E_{11}^{(2)}(E_{22k}) - E_{11(I)}}{E_{11(I+1)} - E_{11(I)}} \tag{48}$$

with $E_{11}^{(2)}(E_{22k})$ also assumed and improved iteratively and $I\,(k)$ is the interval addressed for each $k$. Thereafter, $\omega'_{33}(E_{33})$ is directly given by Eq. (35).

Finally, Eqs. (37) and (39) are used to update $E_{11}^{(2)}(E_{22})$ and $E_{11}^{(3)}(E_{33})$ (i.e. $\{E_{22}, E_{11}^{(2)}\}$ and $\{E_{33}, E_{11}^{(3)}\}$) for the next iteration. Just consider them in terms of the selected basic strain functions after applying the incompressibility conditions (38), e.g.

$$\omega'_{11}(E_{11}^{(2)}(E_{22})) = \omega'_{33}(-E_{22} - E_{11}^{(2)}(E_{22})) \tag{49}$$

and take the derivative respect to the main argument

$$\omega''_{11}(E_{11}^{(2)}(E_{22}))\frac{dE_{11}^{(2)}}{dE_{22}} = \omega''_{33}(-E_{22} - E_{11}^{(2)}(E_{22})) \left(-1 - \frac{dE_{11}^{(2)}}{dE_{22}}\right) \tag{50}$$

where in this case we make the following definitions

$$\begin{cases} \omega''_{11}(E^{(2)}_{11}(E_{22})) := \left.\dfrac{d\omega'_{11}(E_{11})}{dE_{11}}\right|_{E_{11}=E^{(2)}_{11}(E_{22})} \\ \omega''_{33}(-E_{22}-E^{(2)}_{11}(E_{22})) := \left.\dfrac{d\omega'_{33}(E_{33})}{dE_{33}}\right|_{E_{33}=-E_{22}-E^{(2)}_{11}(E_{22})} \end{cases} \tag{51}$$

Then

$$\frac{dE^{(2)}_{11}(E_{22})}{dE_{22}} = -\frac{\omega''_{33}(-E_{22}-E^{(2)}_{11}(E_{22}))}{\omega''_{11}(E^{(2)}_{11}(E_{22}))+\omega''_{33}(-E_{22}-E^{(2)}_{11}(E_{22}))} \tag{52}$$

where the derivatives are computed from the chain rule; for example

$$\frac{d\omega'_{11}(E_{11})}{dE_{11}} = \frac{d\omega'_{11}(\xi_1(E_{11}))}{d\xi_1}\frac{d\xi_1}{dE_{11}} = \frac{1}{h_1}\frac{d\omega'_{11}(\xi_1(E_{11}))}{d\xi_1} \tag{53}$$

where $h_1 = E_{11(I+1)} - E_{11(I)}$ is the discretization in direction 11. A spline function $\{E_{22}, dE^{(2)}_{11}(E_{22})/dE_{22}\}$ may be constructed in order to integrate it and obtain an updated guess $\{E_{22}, E^{(2)}_{11}(E_{22})\}$. A similar procedure is applied with the other equation to obtain $\{E_{33}, E^{(3)}_{11}(E_{33})\}$ with

$$\frac{dE^{(3)}_{11}(E_{33})}{dE_{33}} = -\frac{\omega''_{22}(-E_{33}-E^{(3)}_{11}(E_{33}))}{\omega''_{11}(E^{(3)}_{11}(E_{33}))+\omega''_{22}(-E_{33}-E^{(3)}_{11}(E_{33}))} \tag{54}$$

where similar definitions apply for $\omega''_{ii}$. Then, after both transverse strain functions have been updated, a new iteration is performed. See further details of this type of procedure in Ref. [5].

*4.2. A general computational scheme*

To arrive at a more general and systematic procedure, consider the system of equilibrium and compatibility differential Equations (34) to (39) in residual form

$$\begin{cases} R_1 = \omega'_{11}(E_{11}) - \omega'_{22}(E^{(1)}_{22}(E_{11})) - \sigma_{11}(E_{11}) \\ R_2 = \omega'_{22}(E_{22}) - \omega'_{11}(E^{(2)}_{11}(E_{22})) - \sigma_{22}(E_{22}) \\ R_3 = \omega'_{22}(E^{(1)}_{22}(E_{11})) - \omega'_{33}(-E_{11}-E^{(1)}_{22}(E_{11})) \\ R_4 = \omega'_{11}(E^{(2)}_{11}(E_{22})) - \omega'_{33}(-E_{22}-E^{(2)}_{11}(E_{22})) \\ R_5 = \omega'_{11}(E^{(3)}_{11}(E^{(3)}_{22})) - \omega'_{22}(E^{(3)}_{22}) \end{cases} \tag{55}$$

where the known functions are (data from the tests)

$$\sigma_{11}(E), \sigma_{22}(E), E_{22}^{(1)}(E) \tag{56}$$

and the unknown ones

$$\omega'_{11}(E), \omega'_{22}(E), \omega'_{33}(E), E_{11}^{(2)}(E), E_{11}^{(3)}(E) \tag{57}$$

Using spline interpolations, for all the functions, these equations, at each possible evaluation point $k_1$, $k_2$, $k_3$ (where the subindex implies the discretization employed for each test) may be written in compact form as

$$R_{1k_1} = \left[P\left(\xi_1\left(E_{11k_1}\right)\right)\right]\{\varpi_{11}\} - \left[P\left(\xi_1\left(E_{22}^{(1)}\left(E_{11k_1}\right)\right)\right)\right]\{\varpi_{22}\} - \left[P\left(\xi_1\left(E_{11k_1}\right)\right)\right]\{\bar{\sigma}_{11}\} \tag{58}$$

$$R_{2k_2} = \left[P\left(\xi_2\left(E_{22k_2}\right)\right)\right]\{\varpi_{22}\} - \left[P\left(\xi_2\left(E_{11}^{(2)}\left(E_{22k_2}\right)\right)\right)\right]\{\varpi_{11}\} - \left[P\left(\xi_2\left(E_{22k_2}\right)\right)\right]\{\bar{\sigma}_{22}\} \tag{59}$$

$$R_{3k_1} = \left[P\left(\xi_1\left(E_{22}^{(1)}\left(E_{11k_1}\right)\right)\right)\right]\{\varpi_{22}\} - \left[P\left(\xi_1(-E_{11k_1} - E_{22}^{(1)}\left(E_{11k_1}\right))\right)\right]\{\varpi_{33}\} \tag{60}$$

$$R_{4k_2} = \left[P\left(\xi_2\left(E_{11}^{(2)}\left(E_{22k_2}\right)\right)\right)\right]\{\varpi_{11}\} - \left[P\left(\xi_2\left(-E_{22k_2} - E_{11}^{(2)}\left(E_{22k_2}\right)\right)\right)\right]\{\varpi_{33}\} \tag{61}$$

$$R_{5k_3} = \left[P\left(\xi_3\left(E_{11}^{(3)}\left(E_{22k_3}\right)\right)\right)\right]\{\varpi_{11}\} - \left[P\left(\xi_3\left(E_{22k_3}\right)\right)\right][\varpi_{22}] \tag{62}$$

where

$$E_{11}^{(i)}\left(E_{22k_i}\right) = \left[P\left(\xi_i\left(E_{22k_i}\right)\right)\right]\left\{\bar{E}_{11}^{(i)}\right\},\ i = 1, 2, 3$$

In these equations the normalized abscissae in an interval $I\,(k_1)$, $J\,(k_2)$, $K\,(k_3)$ are obtained, for example as

$$\xi_1\,(E) = \frac{E - E_{11(I)}}{E_{11(I+1)} - E_{11(I)}} \quad \text{with} \quad E_{11(I)} \leq E < E_{11(I+1)} \tag{63}$$

where $I$ may take the values $1, ..., N_1$. The system of nonlinear equations may be written as the function

$$\left\{\mathsf{R}\left(\varpi_{11}, \varpi_{22}, \varpi_{33}, \bar{E}_{11}^{(2)}, \bar{E}_{11}^{(3)}\right)\right\} \longrightarrow \{0\} \tag{64}$$

Assuming that the system of equations is well conditioned (i.e. independent tests and the same number of independent equations than unknowns), the solution is unique. To achieve this, we can take, for example, $N_1 = N_2 = N_3 = N$. The values of $E_{11k_1}$ and $E_{22k_2}$ may be the values at the nodes in each axis, so in this case we get the nodal value simplifications

$$\left[P\left(\xi_1\left(E_{11k_1}\right)\right)\right]\left\{\varpi_{11}\right\} = \varpi_{11k_1} \quad \text{and} \quad \left[P\left(\xi_2\left(E_{22k_2}\right)\right)\right]\left\{\varpi_{22}\right\} = \varpi_{22k_2} \tag{65}$$

$$\left[P\left(\xi_1\left(E_{11k_1}\right)\right)\right]\left\{\bar{\sigma}_{11}\right\} = \bar{\sigma}_{11k_1} \text{ and } \left[P\left(\xi_2\left(E_{22k_2}\right)\right)\right]\left\{\bar{\sigma}_{22}\right\} = \bar{\sigma}_{22k_2} \tag{66}$$

The system of equations may also be solved in minimum squares sense minimizing $\{\mathsf{R}\}^T\{\mathsf{R}\}$. If the selected method to solve the nonlinear equations needs the gradient, it can be easily computed by the chain rule because the functions are just local polynomials. Since the math is lengthy but otherwise straightforward and standard, we omit the details.

The performance of every iterative procedure depends on the initial guess, and the general procedure requires an initial guess in all unknowns. A good starting guess may be obtained for this type of problem, for example, by (see [5])

$$E_{11}^{(2)}\left(E_{22}\right) = -\nu_{21}E_{22} \tag{67}$$

$$E_{11}^{(3)}\left(E_{33}\right) = -\nu_{31}E_{33} \tag{68}$$

and

$$\omega_{11}'\left(E_{11}\right) = \sigma_{11}\left(E_{11}\right), \quad \omega_{22}'\left(E_{22}\right) = \sigma_{22}\left(E_{22}\right) \tag{69}$$

$$\omega_{33}'\left(-E_{11} - E_{22}^{(1)}\left(E_{11}\right)\right) = \sigma_{22}\left(E_{22}^{(1)}\left(E_{11}\right)\right) \tag{70}$$

where $\nu_{21}$ and $\nu_{31}$ are the infinitesimal Poisson ratios. Guesses (69) come from the observation that the overall shapes of stored energy derivative terms are similar to those of the experimental stresses. For example, the second addend in Eq. (27) is usually significantly smaller that the first addend; similar observations are obtained from Eqs. $(55)_1$ and $(55)_2$. Guess (70), obtained for each value $E_{11}$, is obtained from Eq. $(55)_3$ upon the consideration of Eq. $(69)_2$.

We note that the equations of different complete sets of tests proposed to determine the stored energies are also different, so Eqs. (55) will also be different. However, the same procedure may be easily employed for any other complete set of tests proposed, just after establishing the differential equations for the tests as we did for this case in Eqs. (55) as an example. In summary, the general procedure

consists of the following steps

1. Obtain the differential equations of the complete set of tests, as in Eqs. $(55)_1$–$(55)_3$, using known experimental data as in Eqs. (56), so the stored energy is uniquely determined. Note that, as in Eqs. (55), additional unknown functions ($E_{11}^{(2)}(E), E_{11}^{(3)}(E)$ in that case) may be needed. In such case, the addition of compatibility equations is required, i.e. Eqs. $(55)_4$ and $(55)_5$
2. The set of unknown functions, Eq. (57), can be solved numerically using the equilibrium and compatibility Eqs. (55). To this end, the equations are discretized using piecewise spline interpolations, Eqs. (58)–(62).
3. The nodal values for the piecewise spline interpolations are computed solving the nonlinear system of equations (64).
4. The converged nodal values, can be used to build the final energy interpolations, Eqs. (33), which are passed to the finite element program.

We note that frequently, depending on the proposed tests, some energy terms may be computed explicitly, as it is usually the case for the shear $\omega'_{ij}$ $(i \neq j)$ terms, see [18].

Finally we want to remark that the forms of Eqs. (25) and (32) are not a restriction of the WYPiWYG procedures. These forms are an extrapolation of the similar uncoupling found in the infinitesimal limit, so the theory is compatible with that limit. Of course more general solutions of the form

$$\mathcal{W}\left(E_{11}, E_{22}, E_{33}, E_{12}^2, E_{23}^2, E_{31}^2\right) \tag{71}$$

would be possible in the present framework if multidimensional spline interpolation surfaces are employed and the corresponding equilibrium equations are discretized as explained in this section. However we note that a general form of the type Eq. (71), include couplings between strains. The experiments needed to determine such couplings include, for example, a family of uniaxial tests giving $\sigma_{11}\left(E_{11}\right)$ for different combinations of the remaining strains $E_{22}$ and $E_{33}$. To the best of the authors' knowledge, there is not such a complete set of tests in the literature for any material which may allow the determination of a general function of the type Eq. (71) without any assumption. Then, Eqs. (25) and (32) constitute a compromise which, we note, it is compatible with the infinitesimal theory at all strain levels, and includes all invariants except the coupled invariant $E_{12}E_{23}E_{13}$.

*4.3. Six simple shear tests with additional (required) tests*

The governing equation of a simple shear test in the preferred plane $n-t$, with $n$ indicating the glide plane and $t$ indicating the direction of shearing, is [29], [17]

$$\sigma_{nt}(\gamma) = \frac{1}{2}\sin(2\psi)\left(\cos(2\psi) + E_{nt}\sin(2\psi)\right)\left(\omega'_{nn}(E) - \omega'_{tt}(-E)\right) + (1-E)\sin^2(2\psi)\omega'_{nt}(E_{nt}) \tag{72}$$

with $0 < \gamma < \infty$ the corresponding amount of shear and

$$\psi(\gamma) = \tfrac{1}{2}\arctan(2/\gamma) \tag{73}$$

$$E(\gamma) = -\ln(\tan\psi(\gamma))\cos(2\psi(\gamma)) > 0 \tag{74}$$

$$E_{nt}(\gamma) = -\ln(\tan\psi(\gamma))\sin(2\psi(\gamma)) = E_{tn}(\gamma) > 0 \tag{75}$$

where $\pi/4 = \psi(0) > \psi(\gamma) > \psi(\infty) = 0$. We can write

$$\sigma_{nt}(\gamma) = f(\gamma)\left(\omega'_{nn}(E) - \omega'_{tt}(-E)\right) + g(\gamma)\,\omega'_{nt}(E_{nt}) \tag{76}$$

with

$$f(\gamma) = \frac{1}{2}\sin(2\psi)\left(\cos(2\psi) + E_{nt}\sin(2\psi)\right) \tag{77}$$

$$g(\gamma) = (1-E)\sin^2(2\psi) \tag{78}$$

We note that the indices imply glide plane and direction of shearing, so $\sigma_{tn}$ is the shear stress of a different shear experiment, where the glide plane is $t$ and $n$ is the shearing direction. Obviously during any of these tests, the complementary plane has the same shear stress by equilibrium, so we use the indices to distinguish experiments, not planes in the same experiment.

In the small strain limit, $\psi \to \pi/4$ and $\boldsymbol{E} \to \boldsymbol{\varepsilon}$. Retaining only linear terms in Eq. (76) we arrive at

$$\sigma_{nt}(\gamma) = 2\mu_{nt}\varepsilon_{nt} = \mu_{nt}\gamma \tag{79}$$

If in both shear tests we consider the same amount of shear $\gamma$, we have $\gamma = 2\varepsilon_{nt} = 2\varepsilon_{tn}$. Since in the infinitesimal case $\mu_{nt} = \mu_{tn}$ we have

$$\sigma_{tn}(\gamma) = 2\mu_{nt}\varepsilon_{tn} = 2\mu_{nt}\varepsilon_{nt} = \sigma_{nt}(\gamma) \tag{80}$$

so only three shear responses in preferred planes are independent, i.e. one per each preferred plane, regardless of the direction of shearing, as it is well-known.

However, when large strains are considered, for the same amount of shear we still have $E_{tn}(\gamma) = E_{nt}(\gamma)$, but in general $\sigma_{tn}(\gamma) \neq \sigma_{nt}(\gamma)$, so Eq. (76) gives in general

a different response than

$$\sigma_{tn}(\gamma) = f(\gamma)\left(\omega'_{tt}(E) - \omega'_{nn}(-E)\right) + g(\gamma)\,\omega'_{nt}(E_{nt}) \tag{81}$$

at the same shear strain level $\gamma > 0$. Thus, six different shear responses in preferred planes are obtained in general for the large strain case, i.e. one per each preferred plane *and* shearing direction. However, it can be easily shown that for the same amount of shear $\gamma > 0$ we have

$$\sigma_{12}(\gamma) - \sigma_{21}(\gamma) + \sigma_{23}(\gamma) - \sigma_{32}(\gamma) + \sigma_{31}(\gamma) - \sigma_{13}(\gamma) = 0 \tag{82}$$

so in fact *only five*, out of the six different simple shear responses in preferred planes, are independent.

Six shear tests in preferred planes do not constitute a complete set of experimental data from which a generally orthotropic finite strain nonlinear model, compatible with the corresponding infinitesimal theory, can be completely determined. Additional experimental tests are required. Holzapfel and Ogden [7] mention the limitations of biaxial data alone in order to determine an orthotropic material because the corresponding biaxial response curves can be captured by a transversely isotropic model, so a need of additional experimental tests is suggested therein. In the same line, for ventricular myocardium, a set of six simple shear responses are neither sufficient to determine an orthotropic material. We show next that these tests, even being rather complete for what it is usually available in soft tissues, they can also be captured by an infinite number of nonlinear orthotropic models compatible with the infinitesimal theory. That is, they are also limited, so we need to assume additional curves to properly define the material behavior. Indeed, in the small strain limit, the three resulting independent shear responses would determine the three shear moduli $\mu_{12}$, $\mu_{23}$ and $\mu_{31}$. Even in the infinitesimal case, it is apparent that three additional independent experimental tests, e.g. uniaxial in preferred directions, are required to determine the remaining axial deviatoric moduli $\mu_{11}$, $\mu_{22}$ and $\mu_{33}$.

Considering finite strains, we note that we can simultaneously solve five (inde-

pendent) equations of the following set of six simple shear equations

$$\sigma_{12}(\gamma) = f(\gamma)(\omega'_{11}(E) - \omega'_{22}(-E)) + g(\gamma)\omega'_{12}(E_{nt}) \tag{83}$$
$$\sigma_{21}(\gamma) = f(\gamma)(\omega'_{22}(E) - \omega'_{11}(-E)) + g(\gamma)\omega'_{12}(E_{nt}) \tag{84}$$
$$\sigma_{23}(\gamma) = f(\gamma)(\omega'_{22}(E) - \omega'_{33}(-E)) + g(\gamma)\omega'_{23}(E_{nt}) \tag{85}$$
$$\sigma_{32}(\gamma) = f(\gamma)(\omega'_{33}(E) - \omega'_{22}(-E)) + g(\gamma)\omega'_{23}(E_{nt}) \tag{86}$$
$$\sigma_{31}(\gamma) = f(\gamma)(\omega'_{33}(E) - \omega'_{11}(-E)) + g(\gamma)\omega'_{31}(E_{nt}) \tag{87}$$
$$\sigma_{13}(\gamma) = f(\gamma)(\omega'_{11}(E) - \omega'_{33}(-E)) + g(\gamma)\omega'_{31}(E_{nt}) \tag{88}$$

for any given set of (pure) shear functions $\omega'_{12}$, $\omega'_{23}$ and $\omega'_{31}$ and any other given additional hypothesis over an axial branch. For example, if we assume that a given preferred direction, say direction 3, is matrix-dominated, then a symmetrizing assumption of the type $\omega'_{33}(E) = -\omega'_{33}(-E)$ may be considered, see [8]. In this last case, we obtain the following explicit solution for the remaining five independent axial branches in terms of the five selected experimental responses—we omit, for convenience in the examples below, the response curve $\sigma_{32}(\gamma)$

$$\omega'_{11}(E) = \frac{1}{2}(\hat{\sigma}_{21}(\gamma) - \hat{\sigma}_{23}(\gamma) - \hat{\sigma}_{31}(\gamma) + 2\hat{\sigma}_{13}(\gamma)) \tag{89}$$
$$\omega'_{11}(-E) = \frac{1}{2}(-\hat{\sigma}_{21}(\gamma) + \hat{\sigma}_{23}(\gamma) - \hat{\sigma}_{31}(\gamma)) \tag{90}$$
$$\omega'_{22}(E) = \frac{1}{2}(\hat{\sigma}_{21}(\gamma) + \hat{\sigma}_{23}(\gamma) - \hat{\sigma}_{31}(\gamma)) \tag{91}$$
$$\omega'_{22}(-E) = \frac{1}{2}(-2\hat{\sigma}_{12}(\gamma) + \hat{\sigma}_{21}(\gamma) - \hat{\sigma}_{23}(\gamma) - \hat{\sigma}_{31}(\gamma) + 2\hat{\sigma}_{13}(\gamma)) \tag{92}$$
$$\omega'_{33}(E) = \frac{1}{2}(-\hat{\sigma}_{21}(\gamma) + \hat{\sigma}_{23}(\gamma) + \hat{\sigma}_{31}(\gamma)) \tag{93}$$

where

$$\hat{\sigma}_{nt}(\gamma) = \frac{\sigma_{nt}(\gamma) - g(\gamma)\omega'_{nt}(E_{nt}(\psi(\gamma)))}{f(\gamma)} \tag{94}$$

with the shear functions $\omega'_{nt}(E) \equiv \omega'_{tn}(E)$ being previously obtained from other tests, e.g. pure shear tests [18], or assumed as we do in the example below.

Finally, since all the arguments of the strain energy terms in Eqs. (83)-(88) are known for a given amount of shear deformation $\gamma > 0$, this system of nonlinear continuum equations can be solved as a linear system of algebraic equations once four branches are known from other tests (or realistically assumed based on physical reasoning) and a discretization in terms of piecewise spline functions is proposed for

the remaining five branches to be determined from the simple shear tests. To do this, consider first the symmetrizing assumption $\omega'_{33}(E) = -\omega'_{33}(-E)$. Then, from Eqs. (83), (84), (85), (87) and (88) expressed in terms of a common logarithmic strain axial component $0 \leq E \leq E_{\max}$ as the basic variable for all the equations

$$\omega'_{11}(E) - \omega'_{22}(-E) = \hat{\sigma}_{12}(E) \tag{95}$$
$$\omega'_{22}(E) - \omega'_{11}(-E) = \hat{\sigma}_{21}(E) \tag{96}$$
$$\omega'_{22}(E) + \omega'_{33}(E) = \hat{\sigma}_{23}(E) \tag{97}$$
$$\omega'_{33}(E) - \omega'_{11}(-E) = \hat{\sigma}_{31}(E) \tag{98}$$
$$\omega'_{11}(E) + \omega'_{33}(E) = \hat{\sigma}_{13}(E) \tag{99}$$

Upon the discretization of each interval $0 \leq E \leq E_{\max}$ in $N+1$ equispaced nodes, we obtain five piecewise functions $\omega'_{11}(E)$, $\omega'_{11}(-E)$, $\omega'_{22}(E)$, $\omega'_{22}(-E)$ and $\omega'_{33}(E)$ as

$$\left.\begin{aligned}
\omega'^{(+)}_{11i}(\xi) &= \sum_{j=1}^{N+1} P_{ij}(\xi)\, \varpi^{(+)}_{11j} \\
\omega'^{(-)}_{11i}(\xi) &= \sum_{j=1}^{N+1} P_{ij}(\xi)\, \varpi^{(-)}_{11j} \\
\omega'^{(+)}_{22i}(\xi) &= \sum_{j=1}^{N+1} P_{ij}(\xi)\, \varpi^{(+)}_{22j} \\
\omega'^{(-)}_{22i}(\xi) &= \sum_{j=1}^{N+1} P_{ij}(\xi)\, \varpi^{(-)}_{22j} \\
\omega'^{(+)}_{33i}(\xi) &= \sum_{j=1}^{N+1} P_{ij}(\xi)\, \varpi^{(+)}_{33j}
\end{aligned}\right\} \quad i = 1, ..., N \tag{100}$$

which include $5 \times (N+1)$ unknowns. Introducing these interpolation functions into Eqs. (95)-(99), and noticing that all of them are evaluated at $E_k$ or $-E_k$, with $k = 1, ..., N+1$, see Eqs. (65) and (66), we arrive at the system of $5 \times (N+1)$ linear

equations

$$\hat{\sigma}_{12k} = \varpi^{(+)}_{11k} - \varpi^{(-)}_{22k} \tag{101}$$

$$\hat{\sigma}_{21k} = \varpi^{(+)}_{22k} - \varpi^{(-)}_{11k} \tag{102}$$

$$\hat{\sigma}_{23k} = \varpi^{(+)}_{22k} + \varpi^{(+)}_{33k} \tag{103}$$

$$\hat{\sigma}_{31k} = \varpi^{(+)}_{33k} - \varpi^{(-)}_{11k} \tag{104}$$

$$\hat{\sigma}_{13k} = \varpi^{(+)}_{11k} + \varpi^{(+)}_{33k} \tag{105}$$

where we know the experimental (modified) data $\hat{\sigma}_{ijk} = \hat{\sigma}_{ij}(E_k)$ and that can be solved algebraically. In matrix format

$$\{\hat{\sigma}\}_M = [K]_{M\times M}\{\varpi\}_M \tag{106}$$

with $M = 5\times(N+1)$. This system is readily solved to give $\{\varpi\}_M$ and, subsequently, the spline-based axial terms. In passing, note that in this case we can directly obtain the values $\{\varpi\}_M$ from the explicit solution of Eqs. (89)-(93). However, we have generalized the procedure to some extent in order to show how to proceed in case the assumption $\omega'_{33}(E) = -\omega'_{33}(-E)$ does not hold.

## 5. Examples

### *5.1. Incompressible isotropic material: Uniaxial test*

In this simple example, that can be computed easily with both methods, we show that the results of the method with the inversion formula (the Sussman-Bathe procedure) and the present more general procedure without inversion formula give the same results. We capture Ogden's model for isochoric isotropic materials with both WYPiWYG procedures. We take the material constants given in Eq. (32) of [9] —we use here their notation

$$\mu_1 = 1.2069\times10^{-5}\,\mathrm{kg\,cm^{-2}}\ ,\quad \mu_2 = 3.7729\,\mathrm{kg\,cm^{-2}}\ ,\quad \mu_3 = -0.052171\,\mathrm{kg\,cm^{-2}}$$
$$\alpha_1 = 8.3952\ ,\quad \alpha_2 = 1.8821\ ,\quad \alpha_3 = -2.2453 \tag{107}$$

In Figure 1.*a* we compare the functions $\omega'(E)$ from Ogden's model and from both procedures, and in Figure 1.*b* the analytical predictions $\sigma(E)$ given by the Ogden model and the numerical ones from both procedures using $N+1 = 25+1$ points from the curve $\sigma(E)$. All solutions are indistinguishable.

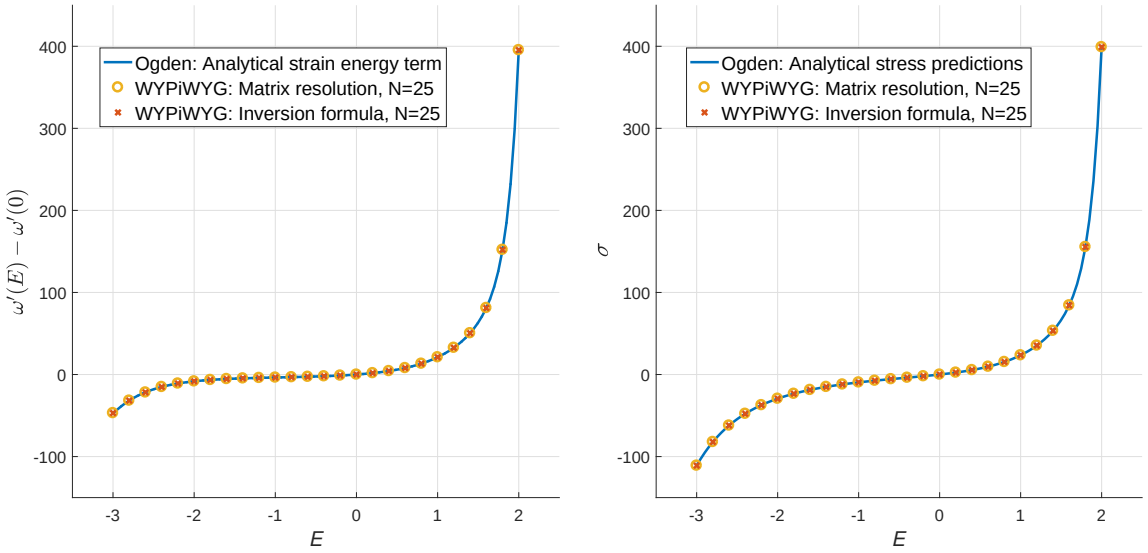


Figure 1: Left (a): First derivative of the Ogden function term $\omega(E)$ using the model parameters of Eq. (107) and both WYPiWYG approximated models with $N = 25$ subdomains. Right (b): Respective uniaxial tension-compression Cauchy stress predictions. Units: $\mathrm{kg}\,/\,\mathrm{cm}^2$.

### *5.2. Incompressible orthotropic material: Simple shear tests*

Consider the simple shear experimental curves in Figure 2, which have been extracted from Figure 7 in Ref. [7] and are presented herein in continuous form. We denote directions $\{f, s, n\}$ of [7] as $\{1, 2, 3\}$. The reader can verify that the curves in that Figure, including the herein omitted curve $\sigma_{32}(\gamma) \simeq \sigma_{31}(\gamma)$, satisfy the general relation of Eq. (82). In this particular case, experimental observation suggests that the relation $\sigma_{32}(\gamma) \simeq \sigma_{31}(\gamma)$ holds for the material under study, but we remark that $\sigma_{32}(\gamma) \neq \sigma_{31}(\gamma)$ in general, as it can be seen in Eqs. (83)-(88). Therefore, we emphasize that we use five curves because only five out of them are independent in general, *and not because* $\sigma_{32}(\gamma) \simeq \sigma_{31}(\gamma)$. In Ref. [7], the dependence on the term $\psi_{8\mathrm{fn}}$ in Eq. (5.27) of Ref. [7] is therein explicitly removed before fitting the data points of Figure 7 of Ref. [7], so that Eqs. (5.27) and Eq. (5.28) therein become the same by model construction. Removing the term $\psi_{8\mathrm{fn}}$ is reasonable in this case because, evidently, experimental data suggests that it must be $\psi_{8\mathrm{fn}} \approx 0$. However, the hypothesis $\psi_{8\mathrm{fn}} \approx 0$ may be a relevant simplification when the experimental data show clearly that $\sigma_{32}(\gamma) \neq \sigma_{31}(\gamma)$, as for example in the experiments given in Figure 5 in Ref. [30]. If that simplification is taken, the general case $\sigma_{32}(\gamma) \neq \sigma_{31}(\gamma)$ cannot be captured. Since we do not take this simplification, we can equally capture the cases when $\sigma_{32}(\gamma) \neq \sigma_{31}(\gamma)$ according to experimental evidence.

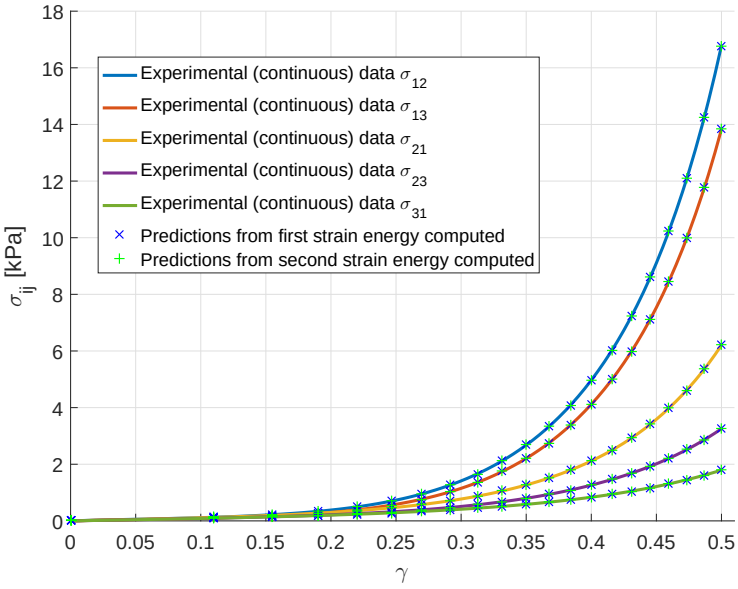


Figure 2: Experimental simple shear stresses and predictions with the two computed stored energy densities.

As mentioned above and it is apparent in the explicit solution given in Eqs. (89)-(93) along with Eq. (94), we need to know the (pure) shear functions $\omega'_{12}$, $\omega'_{23}$ and $\omega'_{31}$ in order to be able to obtain the tension-compression axial functions $\omega'_{11}$, $\omega'_{22}$ and $\omega'_{33}$, where we recall that we also take $\omega'_{33}(E) = -\omega'_{33}(-E)$. Since no additional experimental data is available, we must judiciously assume the shear terms $\omega'_{12}$, $\omega'_{23}$ and $\omega'_{31}$ of our strain energy function. In our opinion, this option is much better, and much more realistic, than just removing the dependence of some invariants in the corresponding strain energy, which may lead to some unexpected results that remain somehow hidden during the fitting procedure [5], [24], but that may affect the confidence in the results obtained during general finite element simulations. In a first (logical) attempt, we have assumed a linear extrapolation from the infinitesimal behavior in terms of logarithmic strains, i.e.

$$\omega'_{ij}(E_{ij}) = 2\mu_{ij}E_{ij} \ , \quad ij = 12, 23, 31 \tag{108}$$

where the shear moduli $\mu_{ij}$ are obtained from the available experimental data as

$$\mu_{ij} = \left.\frac{d\sigma_{ij}}{d\gamma}\right|_{\gamma=0} = \left.\frac{d\sigma_{ji}}{d\gamma}\right|_{\gamma=0} \ , \quad ij = 12, 23, 31 \tag{109}$$

Note that $\mu_{23} = \mu_{31}$ in this particular case.

We discretize now each curve in Figure 2 into $N + 1$ points, which should be equispaced in terms of $E$ and not in terms of $\gamma$, and then solve Eq. (106). We show in Figure 3 both the computed interpolation axial terms and the assumed shear terms. We can see that the axial terms $\omega'_{11}(\pm E)$ and $\omega'_{22}(\pm E)$ have reasonable tendencies, but $\omega'_{33}(E)$ turns negative for the larger strains (note that $E_{\max} \approx 0.06$ for $\gamma_{\max} = 0.5$), which means that the linear relations in terms of logarithmic strains (108) are a good starting point, but must be modified in order to obtain a more realistic solution at large strains. We note, however, that the computed solution, even being no physically plausible, still reproduces *exactly* the experimental data in Figure 2 for $N = 20$, because the solution of Eq. (106) is exact at the selected $M$ points. We show these predictions in Figure 2. In essence, as explained in Refs. [6], [5], a stored energy which fits, even exactly, an incomplete number of tests, does not necessarily represent a good approximation of the actual material behavior in the general loading situation that may appear at integration points in a nonhomogeneous finite element simulation.

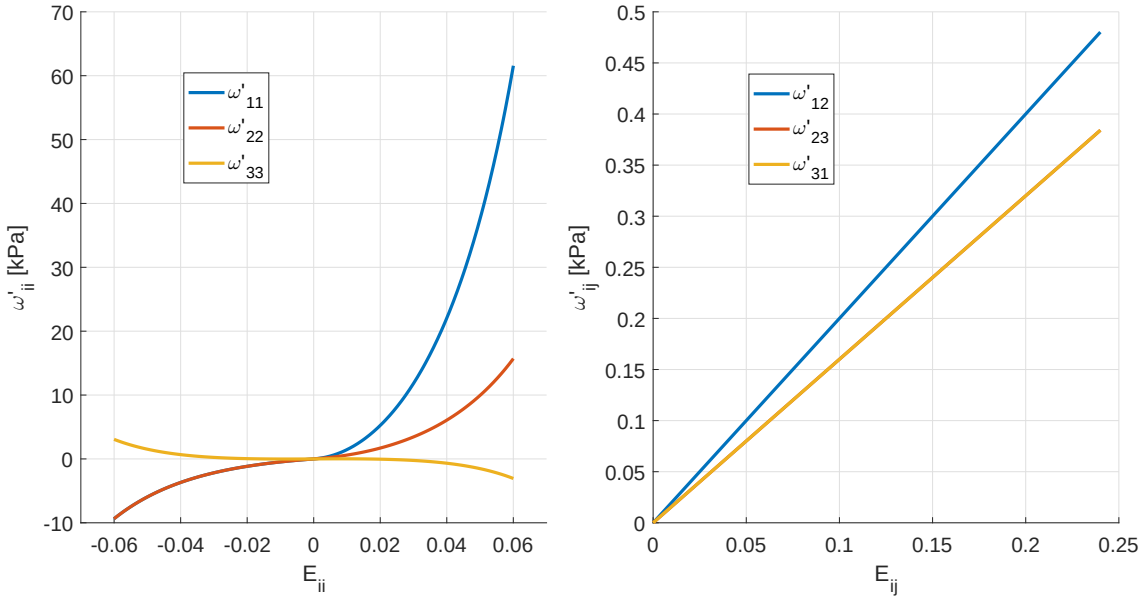


Figure 3: Left (a): Computed strain energy axial terms in the first determination case addressed in this example. Right (b): Assumed strain energy shear terms for the first guess corresponding to linear relations extrapolated from the infinitesimal behavior. The functions $\omega'_{23}(E_{23})$ and $\omega'_{31}(E_{31})$ are coincident due to the fact that $\mu_{23} = \mu_{31}$.

In order to modify the shear terms, we first note that the explicit solution for

$\omega'_{33}(E)$ given in Eq. (93) suggests that one possibility for increasing $\omega'_{33}(E>0)$ is to decrease $\hat{\sigma}_{21}(\gamma>0)$, i.e. to increase $\omega'_{12}(E_{12})$ by means of Eq. (94). Accordingly, and observing also the exponential shape of the experimental responses, we choose an exponential term to each one of the three functions given in Eq. (108), being the added term to $\omega'_{12}(E_{12})$ higher than that for the other two shear functions, see Figure 4.*b*. The exponentially modified terms are —note that $E\exp(bE^4) \simeq E + bE^5 + ...$

$$\omega'_{ij}(E_{ij}) = 2\mu_{ij}E_{ij}\exp(b_{ij}E_{ij}^4) \ , \quad ij = 12, 23, 31 \tag{110}$$

with $b_{12}/b_{31} = 20/3$, $b_{23}/b_{31} = 2$ and $b_{31} = 80$. We show in Figure 4.*a* the computed axial terms in this case, which we herein consider as a possible solution for the material at hand, uniquely determined from the *prescribed* complete set of tests (experimental and assumed). We note that, in contrast to the procedure given in [7], we need to judiciously assume some additional curves, but the available experimental curves, along with the assumed ones, are "exactly" captured regardless of those assumptions. However, whether the model in [7] would predict realistic responses for the missing experimental curves remains unknown. In any case, the response for those missing tests would be already imposed by the model. For the present WYPiWYG procedure, these curves are not arbitrarily imposed (a posteriori) by the set of material parameters obtained fitting the simple shear curves, but prescribed (a priori) by the modeler if they are not available. Of course, if those curves were available, the experimental data would be also captured exactly. We show in Figure 2 the predictions for the experimental simple shear data.

The strain energy determined this way is complete in the sense that it contains the minimum of nine required branches that any nonlinear material model should contain to be compliant with both the finite strain theory and the infinitesimal theory at any strain level. Thus, it will reproduce that theory during finite element simulations under incremental infinitesimal deformations.

We finally note that, as done in [7], we have assumed homogeneous stress fields in the simple shear experiments. However, the aspect ratios of the specimens of the experiments of Dokos et al [26] makes this assumption inaccurate [20], [31], so the proper iterative corrections should be performed [20].

## 6. Conclusion

WYPiWYG hyperelasticity is a family of computational procedures for hyperelasticity initiated by the model of Sussman and Bathe. Traditional hyperelasticity is a semi-inverse method which assumes the global shape of the stored energy function. WYPiWYG hyperelasticity performs local interpolations of stored energy functions,

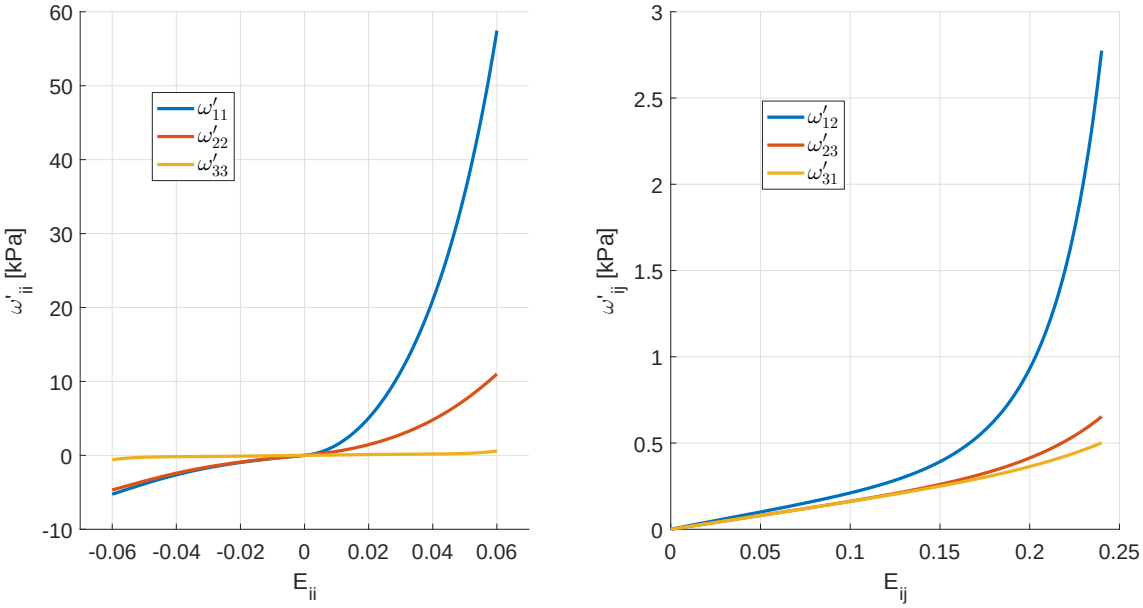


Figure 4: Left (a): Computed strain energy axial terms in the second determination case addressed in this example. Right (b): Assumed strain energy shear terms for the second guess, including linear relations extrapolated from the infinitesimal behavior and additional exponential contributions.

obtaining the stored energy solving numerically the equilibrium equations of a complete set of tests. Thus, the global shapes of the stored energy terms are not assumed, but computed. However, until now, WYPiWYG hyperelasticity was mainly based on an inversion formula in order to solve the differential equations of the uniaxial tests. Thus, the procedure could only be applied in cases were the governing differential equations had an explicit solution, so the method did not have the desired generality.

In this paper we have introduced a more general procedure without the use of the inversion formula that may be employed for any set of tests, regardless of whether the solution of the equilibrium equations is explicit or implicit. In essence, and in the spirit of the Finite Element Method, the method converts a system of ordinary differential equations into a system of discrete algebraic equations, approximating the continuous solution locally. We have shown that this new numerical technique recovers the solution given by the inversion formula. For a practical application, we have determined the stored energy function of passive ventricular myocardium from the usual (limited) set of experimental data curves, which are reproduced to any desired accuracy and for any assumption over the additionally missing tests.

**Acknowledgements**

Partial financial support for this work has been given by grant DPI2015-69801-R from the Dirección General de Proyectos de Investigación of the Ministerio de Economía y Competitividad of Spain. FJM also acknowledges the support of the Department of Mechanical and Aerospace Engineering of University of Florida during the sabbatical period in which this paper was finished and that of Ministerio de Educación, Cultura y Deporte of Spain for the financial support for that stay under grant PRX15/00065.

**References**

[1] KJ Bathe (2014). Finite Element Procedures (2nd Ed). Klaus-Jürgen Bathe, Watertown.

[2] LRG Treloar (1975). The physics of rubber elasticity. Oxford University Press, USA.

[3] JD Humphrey (2013). Cardiovascular solid mechanics: cells, tissues, and organs. Springer Science & Business Media.

[4] RW Ogden (1997). Non-linear elastic deformations. Courier Corporation.

[5] M Latorre, X Romero, FJ Montáns (2016). The relevance of transverse deformation effects in modeling soft biological tissues. International Journal of Solids and Structures, 99, 57-70.

[6] M Latorre, E DeRosa, FJ Montáns (2017). Understanding the need of the compression branch to characterize hyperelastic materials. International Journal of Non-Linear Mechanics, 89, 14-24.

[7] GA Holzapfel, RW Ogden (2009). Constitutive modelling of passive myocardium: a structurally based framework for material characterization. Philosophical Transactions of the Royal Society of London A: Mathematical, Physical and Engineering Sciences, 367(1902), 3445-3475.

[8] KM Moerman, CK Simms, T Nagel (2016). Control of tension–compression asymmetry in Ogden hyperelasticity with application to soft tissue modelling. Journal of the Mechanical Behavior of Biomedical Materials, 56, 218-228.

[9] RW Ogden, G Saccomandi, I Sgura (2004). Fitting hyperelastic models to experimental data. Computational Mechanics, 34(6), 484-502.

[10] FT Stumpf, RJ Marczak (2010). Optimization of constitutive parameters for hyperelastic models satisfying the Baker-Ericksen inequalities. Mecanica Computational, 29, 2901-2916.

[11] K Urayama (2006). An experimentalist's view of the physics of rubber elasticity. Journal of Polymer Science, Part B: Polymer Physics, 44, 3440-3444.

[12] M Destrade, L Dorfmann (2015). Ray W Ogden: An Appreciation. Mathematics and Mechanics of Solids, 20(6), 621-624.

[13] J Crespo, M Latorre, FJ Montáns (2017). WYPIWYG hyperelasticity for isotropic, compressible materials. Computational Mechanics, 59(1), 73-92.

[14] T Sussman, KJ Bathe (2009). A model of incompressible isotropic hyperelastic material behavior using spline interpolations of tension-compression test data. Communications in Numerical Methods in Engineering, 25(1), 53-63.

[15] EA Kearsley, LJ Zapas (1980). Some methods of measurement of an elastic strain-energy function of the Valanis-Landel type. Journal of Rheology, 24(4), 483-500.

[16] KC Valanis, RF Landel (1967). The Strain-Energy Function of a Hyperelastic Material in Terms of the Extension Ratios. Journal of Applied Physics, 38(7), 2997-3002.

[17] M Latorre, FJ Montáns (2013). Extension of the Sussman–Bathe spline-based hyperelastic model to incompressible transversely isotropic materials. Computers & Structures, 122, 13-26.

[18] M Latorre, FJ Montáns (2014). What-You-Prescribe-Is-What-You-Get orthotropic hyperelasticity. Computational Mechanics, 53(6), 1279-1298.

[19] X Romero, M Latorre, FJ Montáns. Determination of the WYPiWYG strain energy density of skin through finite element analysis of the experiments on circular specimens. Under review.

[20] M Latorre, E Peña, FJ Montáns (2016). Determination and finite element validation of the WYPIWYG strain energy of superficial fascia from experimental data. Annals of Biomedical Engineering, in press, DOI: 10.1007/s10439-016-1723-2

[21] JG Murphy (2013). Transversely isotropic biological, soft tissue must be modelled using both anisotropic invariants. European Journal of Mechanics-A/Solids, 42, 90-96.

[22] JG Murphy (2014). Evolution of anisotropy in soft tissue. Proceedings of the Royal Society A, 470(2161), 20130548.

[23] M Destrade, B Mac Donald, JG Murphy, G Saccomandi (2013). At least three invariants are necessary to model the mechanical response of incompressible, transversely isotropic materials. Computational Mechanics, 52(4), 959-969.

[24] JG Murphy, S Biwa (2017). The counterintuitive mechanical response in simple tension of arterial models that are separable functions of the $I_1$, $I_4$, $I_6$ invariants. International Journal of Non-Linear Mechanics, 90, 72-81.

[25] P Skacel, J Bursa (2016). Poisson's ratio of arterial wall–Inconsistency of constitutive models with experimental data. Journal of the Mechanical Behavior of Biomedical Materials, 54, 316-327.

[26] S Dokos, BH Smaill, AA Young, IJ LeGrice (2002). Shear properties of passive ventricular myocardium. American Journal of Physiology-Heart and Circulatory Physiology, 283(6), H2650-H2659.

[27] M Latorre, FJ Montáns (2015). Material-symmetries congruency in transversely isotropic and orthotropic hyperelastic materials. European Journal of Mechanics-A/Solids, 53, 99-106.

[28] M Latorre, FJ Montáns (2016). Stress and strain mapping tensors and general work-conjugacy in large strain continuum mechanics. Applied Mathematical Modelling, 40(5), 3938-3950.

[29] P Chadwick (2012). Continuum mechanics: concise theory and problems. Courier Corporation.

[30] O Gültekin, G Sommer, GA Holzapfel (2016). An orthotropic viscoelastic model for the passive myocardium: continuum basis and numerical treatment. Computer Methods in Biomechanics and Biomedical Engineering, 19(15), 1-18.

[31] M Destrade, JG Murphy, G Saccomandi (2012). Simple shear is not so simple. International Journal of Non-Linear Mechanics, 47(2), 210-214.